Supplementary Material

Methods

Zebrafish

Zebrafish were handled in accordance with EU directive 2011/63/EU as well as the German Animal Welfare Act. The transgenic zebrafish lines (*Tg(sox17:H2B-tBFP), Tg(mezzo:eGFP)*[14] *and Tg(h2afva:h2afva-mCherry)*[15]) were used for visualizing endodermal, mesendodermal and all cells respectively during gastrulation. For obtaining the triple transgenic embryos, a homozygous double transgenic line containing *Tg(mezzo:eGFP) and Tg(h2afva:h2afva-mCherry)* was generated and a female from this line was crossed with a homozygous *Tg(sox17:H2B-tBFP)* male fish. Embryos were collected after fertilization and incubated at 28.5 °C in E3 medium. To generate the *Tg(sox17:H2B-tBFP)* line, the transgene plasmid pTol2-sox17:H2B-tBFP was created by Gibson assembly[27]. The *sox17* promoter was PCR amplified from pSox17:eGFP[28] and cloned into pminiTol2[29,30] to generate pTol2-sox17. The H2B ORF and the tagBFP ORF were PCR amplified and cloned into pTol2-sox17 to generate pTol2-sox17:H2B-tBFP. This plasmid was used to generate the *Tg(sox17:H2B-tBFP)* stable zebrafish line using standard transgenesis protocols[29,30].

Sample preparation

Low-melting agarose (1.5%) solution with fluorescent beads (Merck Estapor fluorescent microspheres FXC-050 1:20000 dilution) was prepared in E3 medium and maintained at 37°C. At high stage, embryos with chorion were transferred into low-melting agarose and sucked into a cleaned FEP tube (inner diameter: 2.0 mm, wall thickness: 0.5 mm), using a micropipette (Eppendorf P200). 3 embryos were positioned on top of each other with minimum gap between them. The agarose was allowed to solidify at room temperature for 5 min and the FEP tube was mounted on the stage, dipping from the top into the sample chamber filled with E3 medium for time-lapse acquisition.

SPIM hardware

A four-lens SPIM setup was used for imaging, consisting of four identical water-dipping Olympus

UMPLFLN 10x/0.3 objectives, two for illumination and two for detection. The sample chamber was custom-made from acrylic with four openings sealed with rubber o-rings. Omicron SOLE-6 laser engine consisting of six different visible laser lines was mounted on the system and the laser beam through fiber was split into two for the two illumination arms. An optical chopper wheel (Thorlabs MC2000B, MC2F57B[a]) was used to generate alternate illumination of the sample from two sides. The chopper wheel provided the start trigger for cameras and stages for image acquisition and its rotation speed was synchronized with the acquisition of the camera. Light sheets were generated with cylindrical lenses and projected with telescopes and the illumination objective lenses onto the common focal plane of both detection lenses. Light sheet thickness was calculated for half width of the field of view and their waists were centered in the respective halves of the FOV, resulting in a wider region with thinner light sheet. A continuously running resonant mirror (1 kHz, EOPC) was used in each illumination arm for even sample illumination (multidirectional SPIM). The average excitation power in the entire object plane was 8 mW per arm. The focal planes of the two detection objectives were imaged onto two Andor Zyla sCMOS cameras through emission filters (Chroma ET 460/50, ET BP525/50, Semrock BP593/46). Both cameras were precisely aligned using a focusable tube lens and an adjustable mirror to acquire images from the same focal plane, which were streamed to separate computers using camera controls implemented in Fiji. The sample was moved and rotated with three motorized linear stages (M-404.1PD/6PD, M-112.1DG) and one rotational stage (M-660.55, Physik Instrumente) using custom-written software in LabView.

Time-lapse acquisition

The setup consists of two illumination arms for dual-sided illumination of the sample and two detection arms to acquire two opposite views covering the entire embryo in ~10 s. The zebrafish embryo was moved along the detection axis through the alternating light sheets to acquire a z-stack of 402 planes. The two cameras were triggered simultaneously every 2 μm, acquiring one image stack for each combination of illumination side and camera, producing four image stacks per channel for each time-point. The laser illuminates the sample only when the entire chip was exposed avoiding any artifacts due to the rolling shutter. These steps were repeated for sequential acquisition of the three channels, which

took 30 s. Time-points were acquired at an interval of 2 mins for a period of 14 h. To image multiple samples in parallel, the stage translated the tube along the y-axis to position the next embryo in front of the objective lenses. By repeating this, a time point is acquired for each sample and the stage moves back to bring the first embryo in the field of view. This entire process is repeated for time-lapse acquisition of multiple samples. In our study, three wildtype embryos were imaged simultaneously.

Fitting a sphere to the transmission image

Before starting the time-lapse acquisition, a single image stack was acquired using transmission light. Due to the limited depth of field, different parts of the embryo were in focus in different planes of the transmission stack. A difference-of-Gaussian approach was used to filter efficiently for these in-focus regions:

$$I'(x,y,z) = |I(x,y,z) - G_\sigma(x,y) * I(x,y,z)|$$

where $I(x,y,z)$ denotes the intensity of the transmission image at pixel (x,y,z), $G_\sigma(x,y)$ is a 2D Gaussian kernel centered at (x,y) with a standard deviation of σ and $*$ denotes plane-wise convolution. Throughout our experiments we used $\sigma = 1$.

Subsequently, a 3x3 median filter was applied to reduce noise. Two spheres were fitted to the resulting image stack by a custom algorithm motivated by the k-means algorithm. First, the image was roughly divided into foreground and background pixels by adjusting a global threshold. Foreground pixels usually covered the surface of the embryo as well as the chorion. Two sphere models were then initialized, both centered at the image center and with estimated radii for the embryo and the chorion, 350µm and 550µm, respectively. An iterative, Expectation-Maximization-like algorithm was then executed, similar to the k-means algorithm: The expectation step assigned each foreground pixel to one of the sphere models, depending on its distance to the spheres' surface. The maximization step updated both sphere models from the assigned pixels using a least-squares fit. Both steps were repeated until convergence. The sphere model with the smaller radius resembled the embryo surface.

Real-time masked raw data acquisition

Since germlayer cells remain close to the surface of the zebrafish embryo throughout the experiment, only the pixels within a certain distance to the surface of the fitted sphere contain information that is of interest for further analysis. Since the position and size of the acquisition volume remain unchanged for all time points, we identify these pixels after sphere fitting and collect their indices, i.e. their linear position within the image stack, in a table. After acquiring each stack, instead of saving the data as ordinary image files, we save a concatenated list of intensity values of the identified pixels. The order of the pixels remains unchanged for consecutive stacks; to reassign intensity values later to pixel positions, we simply save the table with pixel indices once for all time points. This is done for each sample and for each view separately.

Multi-view and time-lapse registration

The four views (image stacks) obtained from combination of two illumination and two detection sides were fused using nonlinear blending to generate a fused image stack based on the transformations pre-calculated with the beads around the sample. This fusion is performed for each time-point in the acquired time-lapse data.

As the embryonic axis forms towards the end of gastrulation, the embryo inside the chorion turns by 90°. To separate this global movement from local cell movements, 3D image stacks of consecutive time points were registered rigidly (Movie 5). For this purpose, the images at each time point were smoothed using a Gaussian kernel with σ=1. Local maxima above a certain threshold (*th* = 150 in our experiments), with neighbor maxima separated by at least 30 gray levels, identified the majority of cells centers. Due to the similarity between images of consecutive time points, our procedure detected a similar subset of cells that were subsequently used to estimate a rigid transformation using the Iterative Closest Point algorithm.

Channel subtraction to separate germ layers

We recorded three transgenic lines (channels) at each time-point, labeling the following layers: Channel 1 recording *Tg(sox17:H2B-tBFP)* expressed in Endoderm (nuclear expression), Channel 2 recording *Tg(mezzo:eGFP)* in Mesoderm + Endoderm (cytoplasmic expression) and Channel 3 recording *Tg(h2afva:h2afva-mCherry)* in Ectoderm + Mesoderm + Endoderm (nuclear expression). By subtracting channel 2 from channel 3 ubiquitously labeling nuclei of all three germ layers, a separate layer with *ectoderm* nuclei was obtained. Likewise, subtracting ectoderm from the channel 3 gave *mesendoderm* layer with nuclear signal and further subtracting endoderm segregated *mesoderm* as well. Channel 1, labeling endoderm nuclei was used as it is for visualizing endoderm. This procedure yielded nuclear signals for all three germ layers. Each layer was then individually segmented and tracked for further analysis.

Data Analysis

Cell tracking

Cells were detected and tracked separately for each germ layer using the TGMM Software[31]. We set the *backgroundThreshold* manually for each layer and sample: (ectoderm /mesoderm/endoderm): sample 1: 30/280/140, sample 2: 350/420/140, and sample 3: 250/150/120. The parameter *anisotropyZ* was set to 1.0, and *thrCellDivisionWithTemporalWindow* to 3.2 for all experiments. All other parameters were left at default values.

Spatial alignment of data sets

Raw tracking results were transformed into a standardized Cartesian coordinate system for each specimen: the origin of this coordinate system was moved to the center of the embryo by subtracting the centroid position of the best-fit sphere from each observed position. The radial position of each cell was then calculated as the length of its (centered) position vector $||(x, y, z)||$. Remaining differences in orientation between datasets were corrected manually by aligning the data with respect to a reference embryo, using the start and end of the movie as well as 75% epiboly stage as reference time points.

Cell counts

Cell numbers n_i for each germ layer were estimated using the number of detected objects at frame i. Relative cell numbers were obtained by normalizing the per-layer cell counts with the total cell number of cells in all three germ layers at each frame i.

Regularity of cell movement

To characterize how *directed* a cell's movement is, we calculated the straightness index[32] (SI) by normalizing the end-to-end distance by the actual path length of a trajectory:

$$SI(\boldsymbol{x}_l) = \frac{||\boldsymbol{x}_l(N_l) - \boldsymbol{x}_l(1)||}{\sum_{i=1}^{N_l-1} ||\boldsymbol{x}_l(i+1) - \boldsymbol{x}_l(i)||}$$

with $||\cdot||$ being the Euclidean norm, $\boldsymbol{x}_l(i)$, being the cell's positions given in a Cartesian coordinate system as $(x_l(i), y_l(i), z_l(i))$, and N_l being the length of the trajectory.

Statistical analysis of cell motion patterns

The influence of different intrinsic and extrinsic factors on straightness of cell motion was first assessed by scatter plots of cell position (mid point of the track) vs. the respective SI of the cell's track, together with the 90% prediction ellipses enclosing the region, where 90% of new observations would be located under the condition that the data is drawn from a bivariate normal distribution.

Correlation of cellular movement across layers

From the vector fields $\overline{\boldsymbol{v}}^{(t)}(\boldsymbol{x})$**,** we calculated circular correlation[33] using the following formula:

$$\rho(\alpha, \beta) = \frac{E\{\sin(\alpha - \mu)\sin(\beta - \nu)\}}{\sqrt{Var(\sin(\alpha - \mu))Var(\sin(\beta - \nu))}}$$

with the circular observations α, β (movement direction at $\boldsymbol{x}$ in radians) and the respective central moments μ and ν. Because μ and ν are not well defined due to the uniform distribution of α, β, we set μ and ν both to 0.

Density weighted streamlines

Flow fields representing directions of cell movement were modified using local cell density estimates. We first projected the cell positions to the unit sphere and mapped the resulting spherical coordinates into the Euclidean plane using the conformal (angle-preserving) Mercator projection. The trajectories where subdivided into 10 intervals in time, each spanning approximately 1.5 hours. The spatial component was discretized using a regular 40x40 grid on the projections. For each single embryo e, we computed a vector field $v_e^{(t)}(\boldsymbol{x})$. The flow vector at each spatial grid cell represents the averaged normalized displacements extracted from all trajectories passing through this particular grid cell during the time interval t. The final flow field $\bar{v}^{(t)}(\boldsymbol{x})$ was obtained by averaging the flow at each grid cell over the samples.

The width of each streamline was then scaled according to the sample count of the grid cell at its starting point. Additionally, we corrected for the area distortion in the Mercator projection, by dividing sample sizes by the area scaling factor $sec^2\phi$ at the respective site $\boldsymbol{x}$, with ϕ being the latitude at the grid point.

Decomposition into movement components

The observed direction of movement $\overline{\boldsymbol{v}}^{(t)}(\boldsymbol{x})$ at each sample point $\boldsymbol{x}$ was decomposed into the proportions associated with epiboly and convergence movement. The decomposition was done according to our previously published method[22]. Briefly: We first constructed reference vector fields representing pure epiboly $\boldsymbol{e}(\boldsymbol{x})$ and convergence movement $\boldsymbol{c}(\boldsymbol{x})$, and projected the actual motion onto the different reference directions: $s_{epi}^{(t)}(\boldsymbol{x}) = < \overline{\boldsymbol{v}}^{(t)}(\boldsymbol{x}), \boldsymbol{e}(\boldsymbol{x}) >$ and $s_{conv}^{(t)}(\boldsymbol{x}) = < \overline{\boldsymbol{v}}^{(t)}(\boldsymbol{x}), \boldsymbol{c}(\boldsymbol{x}) >$ (Extended Data Fig. 6). The actual proportions for each movement component were then given by:

$$p^{(t)}(\boldsymbol{x}) = \begin{cases} 1 - 2\arccos\left(s^{(t)}(\boldsymbol{x})\right), s^{(t)}(\boldsymbol{x}) > \boldsymbol{0} \\ 0, \ else \end{cases},$$

with $s^{(t)} = s_{conv}^{(t)}$ or $s^{(t)} = s_{epi}^{(t)}$. To summarize the fields $p^{(t)}(\boldsymbol{x})$ into a single value per time point we calculated the mean across sites $\boldsymbol{x}$ weighted by the number of observations $w^{(t)}(\boldsymbol{x})$ at $\boldsymbol{x}$:

$$o^{(t)} = \frac{1}{\sum_{\boldsymbol{x}} w^{(t)}(\boldsymbol{x})} \sum_{\boldsymbol{x}} p^{(t)}(\boldsymbol{x})\, w^{(t)}(\boldsymbol{x})$$

3D Rendering of cell positions and trajectories

3D renderings of spherical cell centroids and tubular cell trajectories were created with Blender 2.77. Ambient occlusion was used to improve perception of depth ordering. The camera was set to orthographic to avoid perspective distortions.

Code availability

All the source code (Mathematica Notebooks and Package) is available upon request.

References

27. Gibson, D. G. *et al.* Enzymatic assembly of DNA molecules up to several hundred kilobases. *Nat. Methods* **6,** 343–345 (2009).
28. Mizoguchi, T., Verkade, H., Heath, J. K., Kuroiwa, A. & Kikuchi, Y. Sdf1/Cxcr4 signaling controls the dorsal migration of endodermal cells during zebrafish gastrulation. *Development* **135,** 2521–2529 (2008).
29. Kawakami, K. *et al.* A transposon-mediated gene trap approach identifies developmentally regulated genes in zebrafish. *Developmental Cell* **7,** 133–144 (2004).
30. Clark, K. J., Urban, M. D., Skuster, K. J. & Ekker, S. C. Transgenic zebrafish using transposable elements. *Methods Cell Biol.* **104,** 137–149 (2011).
31. Amat, F. *et al.* Fast, accurate reconstruction of cell lineages from large-scale fluorescence microscopy data. *Nat. Methods* **11,** 951–958 (2014).
32. Batschelet, E. Circular statistics in biology. *Academic Press* (1981).
33. Jammalamadaka, S. R. & Sarma, Y. R. A correlation coefficient for angular variables. *Statistical theory and data analysis II* 349–364 (1988).

Supplementary Figures

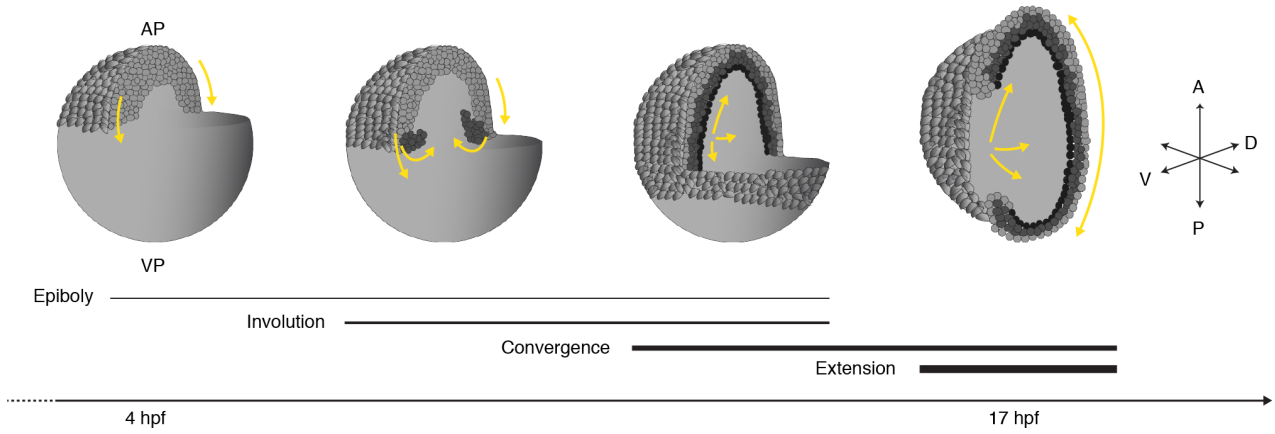

Figure S1: Schematic of gastrulation movements

Schematic showing the temporal overlap of the four major gastrulation movements - epiboly (movement from animal pole to vegetal pole), involution (inward movement), convergence (movement towards the dorsal midline) and extension (movement along the A-P axis).

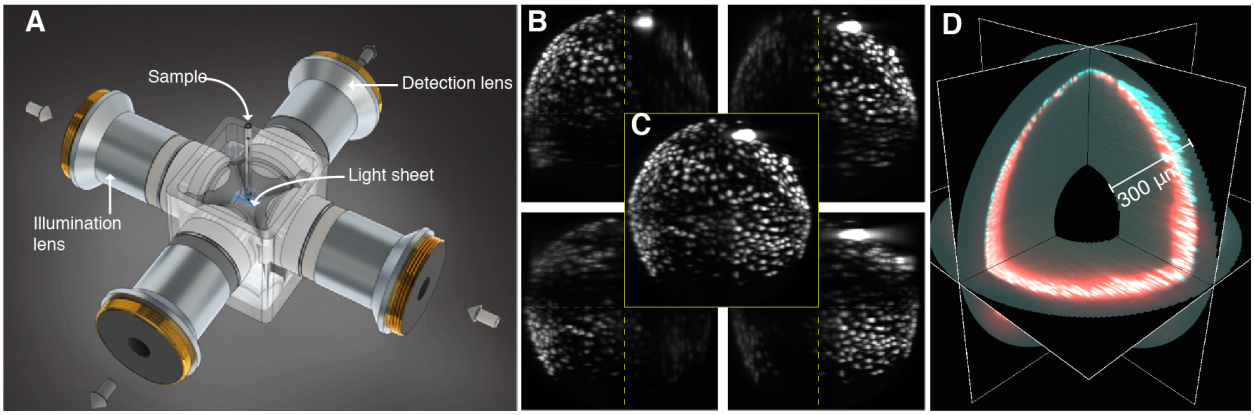

Figure S2: Microscope design and image acquisition

(**A**) The central unit of our 4-lens SPIM setup with two illumination and two detection lenses is shown. The sample is mounted from top, dipping into a water-filled sample chamber. (**B**) shows the four quadrants of raw data acquired by each combination of illumination and detection arm and a fusion of these images is shown in (**C**). (**D**) depicts the acquisition of masked raw data where the center of the embryo consisting of yolk and the blank space outside the embryo is masked to minimize the amount of data acquired. Cut out of the embryo is shown to make the masked black regions and the acquired 300 µm thick shell around the embryo surface visible.

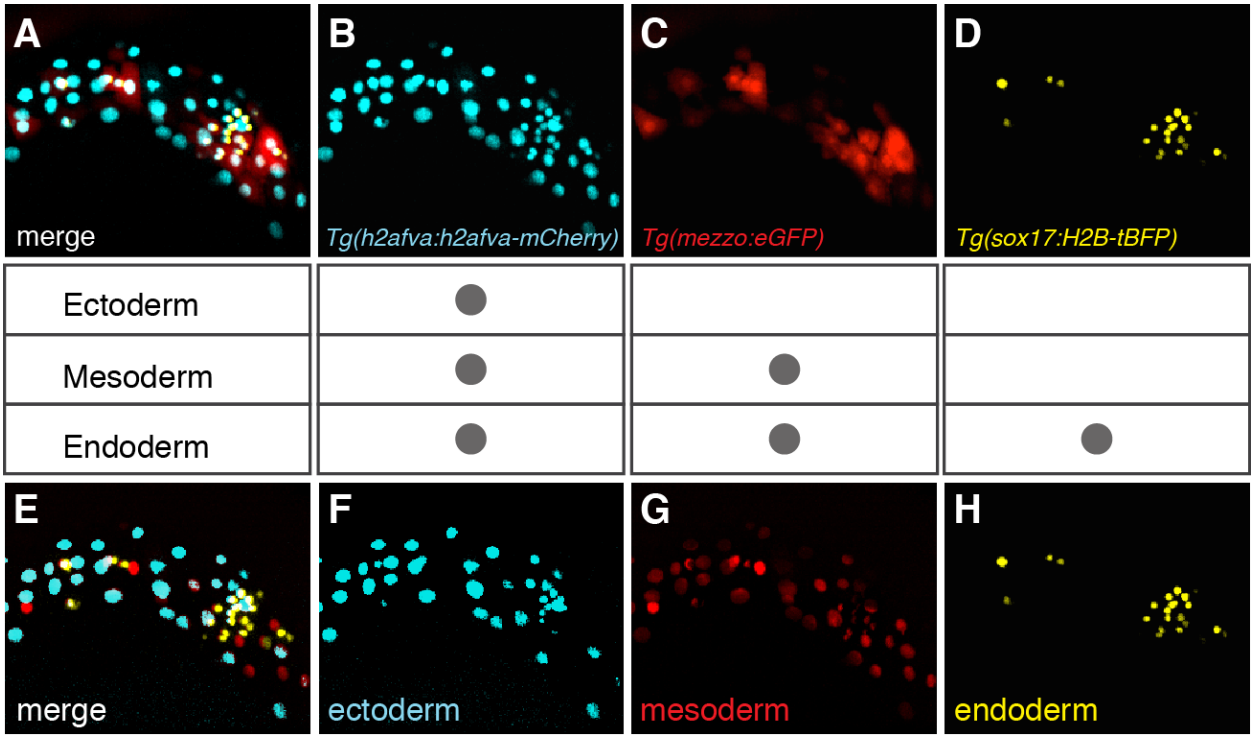

Figure S3: Separation of signal from three transgenes into three germlayers

(**A**) shows the merge of (**B**) *Tg(h2afva:h2afva-mCherry)* labeling nuclei of all cells, (**C**) cytoplasmic marker *Tg(mezzo:eGFP)*, which labels mesendoderm cells and (**D**) *Tg(sox17:H2B-tBFP)* labelling the nuclei of endoderm cells only. (**F-G**) shows the separated nuclear signal of the three germlayers ectoderm, mesoderm and endoderm and their merge is shown in (**E**).

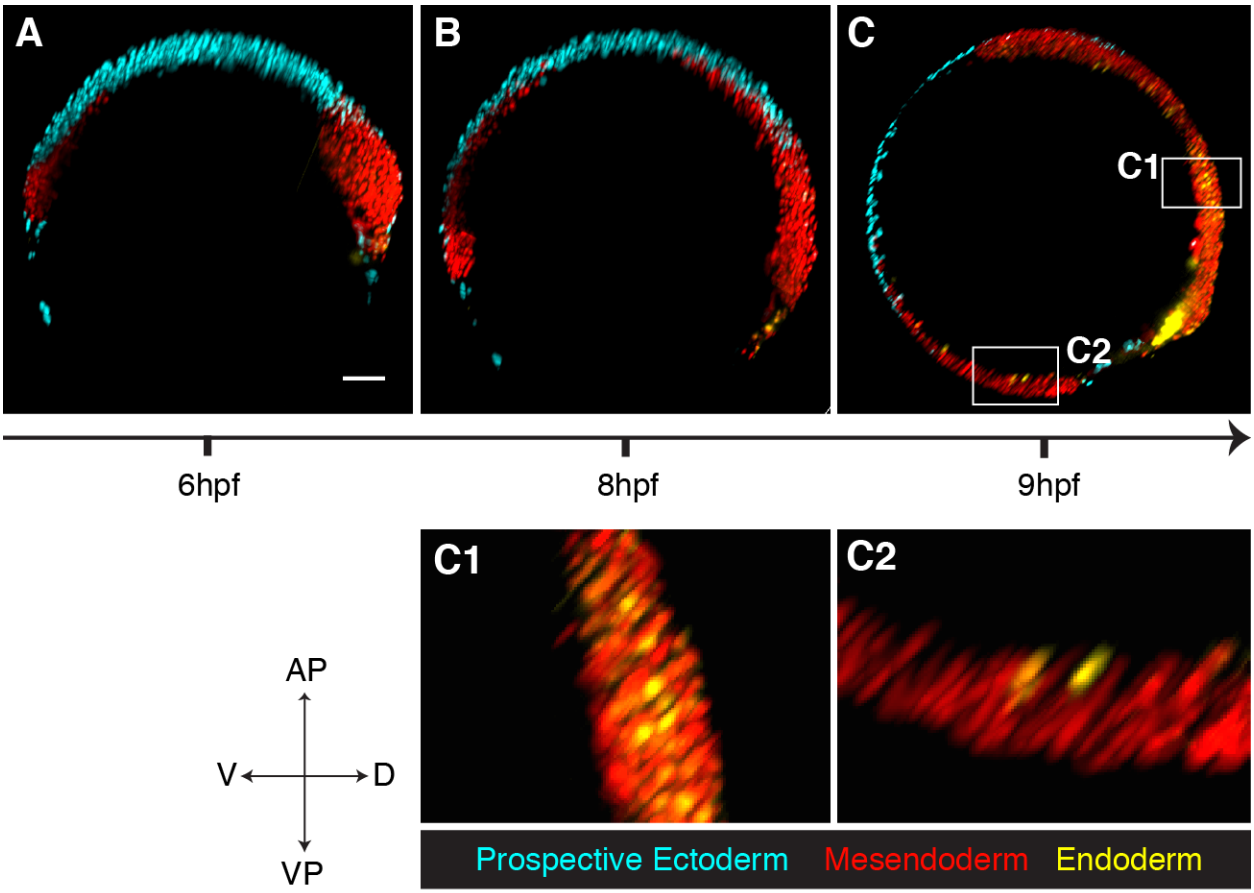

Figure S4: Radial organization of germlayers

(**A-C**) shows the stratification of germlayers. (**A-B**) Cells at the margin invaginate to form a two-layered embryo with outer p. ectoderm (cyan) and inner mesendoderm (red). (**C**) Endoderm (yellow) cells stay mixed with the mesoderm cells (red) until the end of gastrulation and move to a deeper position thereafter (**C1-C2**), giving rise to a three-layered embryo. Scalebar: 100 µm.

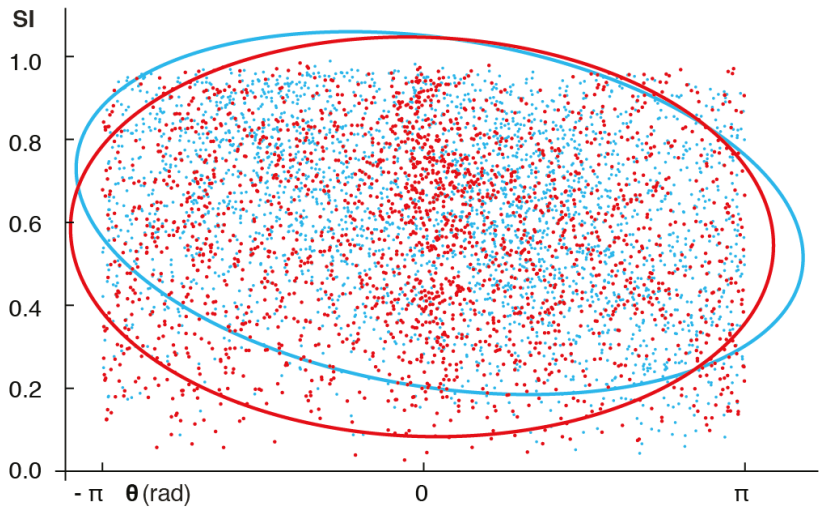

Figure S5: Relationship between straightness of cell migration and longitudinal position. Scatterplot of straightness index vs. longitude position θ (computed at the mid point) for each trajectory (between 4.5 and 7 hpf of mesendoderm (red) and p. ectoderm (blue) and the respective 90% prediction ellipsoids.

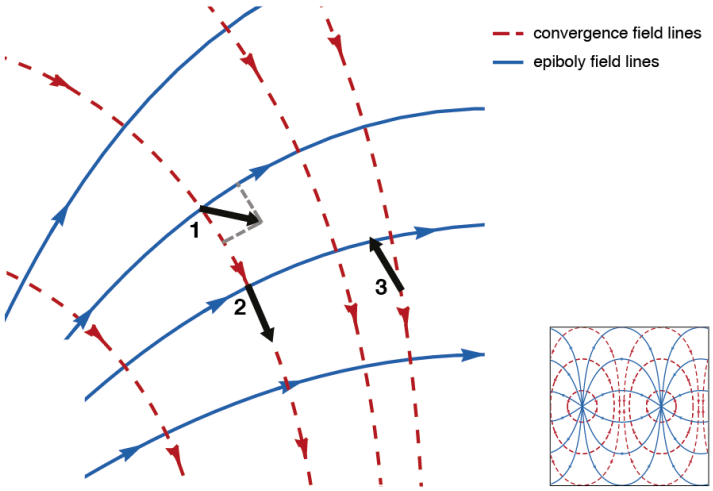

Figure S6: Decomposition of flow directions into morphogenetic movement components.

Reference field lines for convergence (dashed-red) and epiboly (blue) of the region indicated by the box in the inset. The direction of the field lines is indicated by arrows in the respective color. Examples of potential flow directions are shown as black arrows. Dashed lines at arrow 1 indicate the projections onto the epiboly and convergence field lines. Vector 1 points in the direction of both epiboly and convergence, vector 2 solely points in epiboly direction and vector 3 has neither epiboly nor convergence component as it points in the opposite directions.

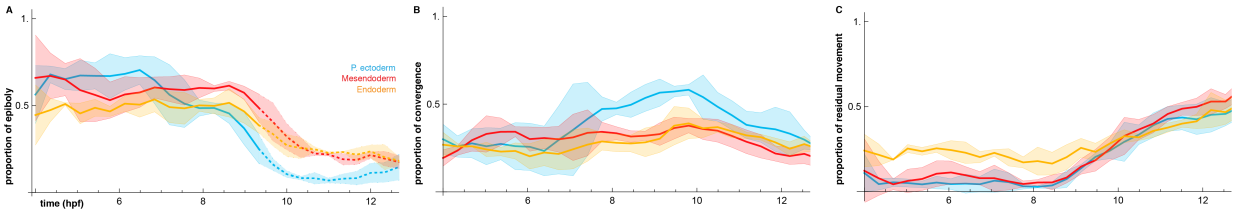

Figure S7: Relative proportions of morphogenetic movements per germlayer.

Average proportions of epiboly (**A**) and convergence (**B**) and residual (**C**) movement for p. ectoderm (blue), mesendoderm (red) and endoderm (yellow): Thick line shows mean (across n=3 embryos) and confidence bands indicate the region of mean +/- 1.96*standard error from 4 to 12.5 hpf. Dashed lines indicate the end of epiboly.

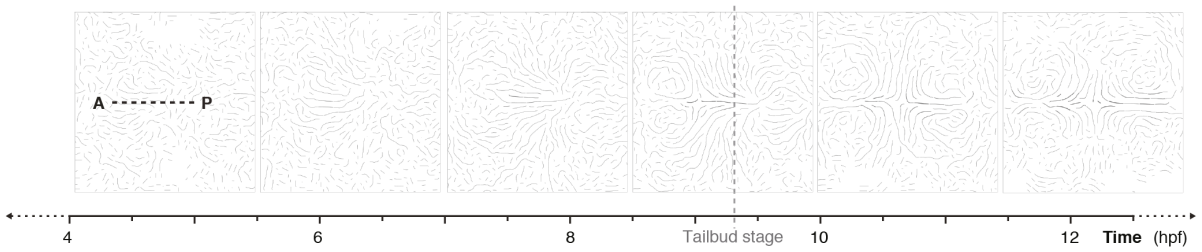

Figure S8: Density weighted streamlines of endodermal layer.

Density weighted streamlines (see Fig. 3E) for endodermal cells. Thickness of streamlines indicates cell density at the respective site. Each interval covers about 1.5 hours of development.

Supplementary movies

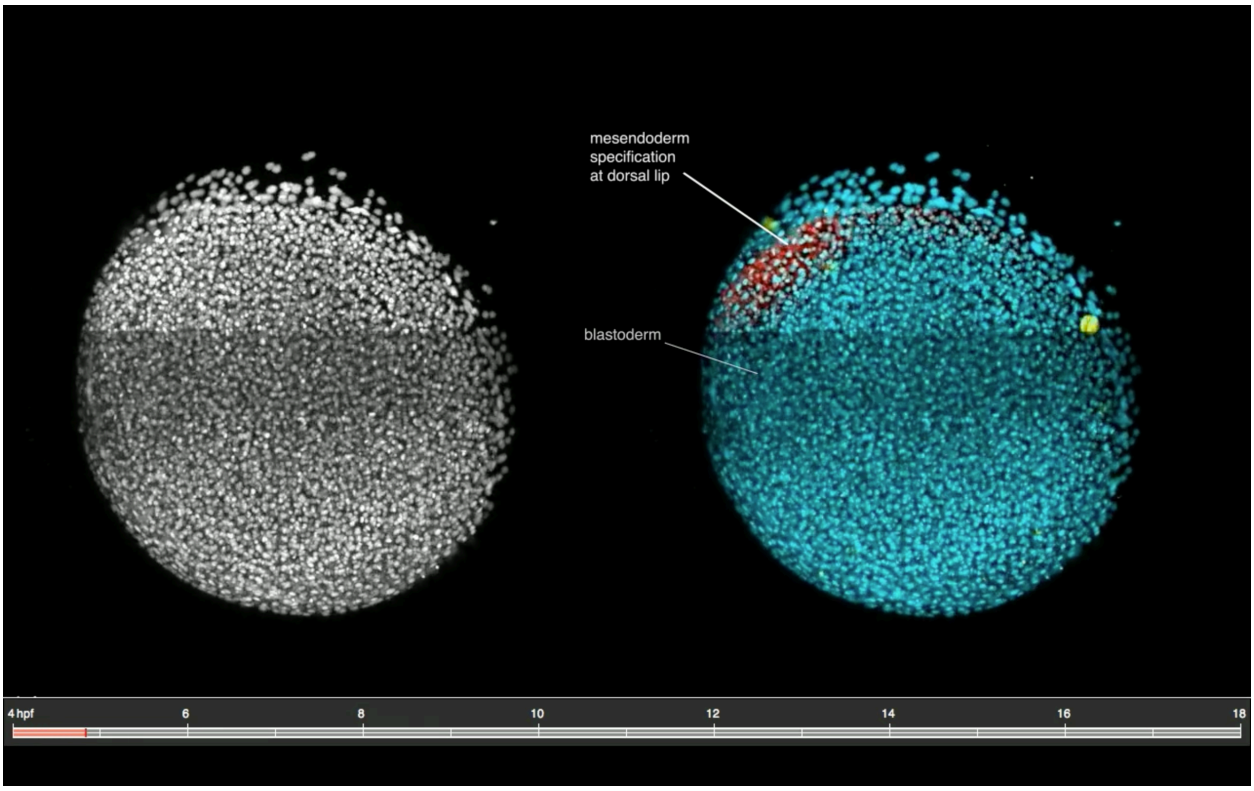

Movie S1: Gastrulation movements and specification of all three germlayers

Tg(h2afva:h2afva-mCherry) embryo labeling nuclei undergoing gastrulation movements from 4-18 hpf is shown (left). Ectoderm (cyan), mesendoderm (red) and endoderm (yellow) identity of the same embryo showing the specification of each germlayer, dynamics and formation of various organs is shown (right). (Submitted videos have been compressed to stay within the file size limits. Higher quality movies are available at https://cloud.mpi-cbg.de/index.php/s/YuKBKB6WPwXRCmA)

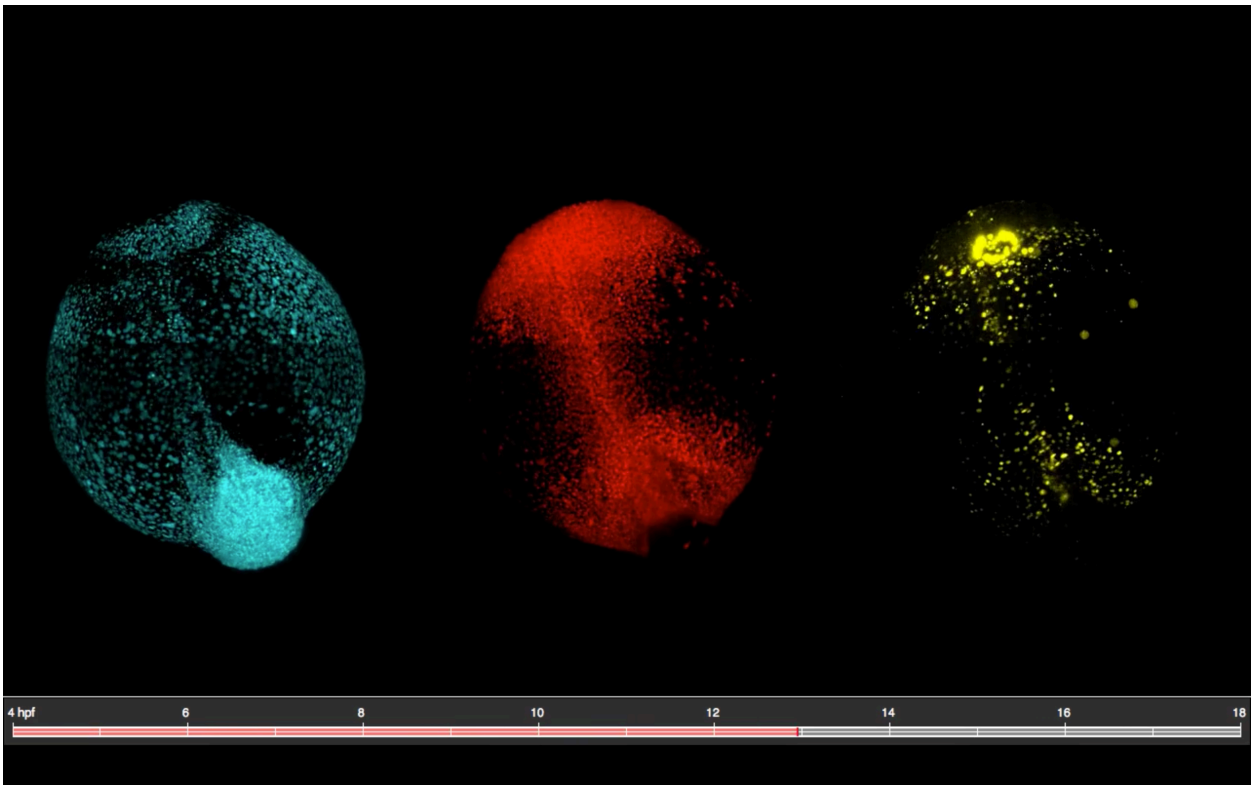

Movie S2: Specification and dynamics of ectoderm, mesoderm and endoderm.

Spatio-temporal dynamics of fate specification showing the formation of ectoderm (cyan), mesendoderm (red) and endoderm (yellow). Dynamics of these germlayers from 4-18 hpf leading to the formation of various organs is shown.

(Submitted videos have been compressed to stay within the file size limits. Higher quality movies are available at https://cloud.mpi-cbg.de/index.php/s/YuKBKB6WPwXRCmA)

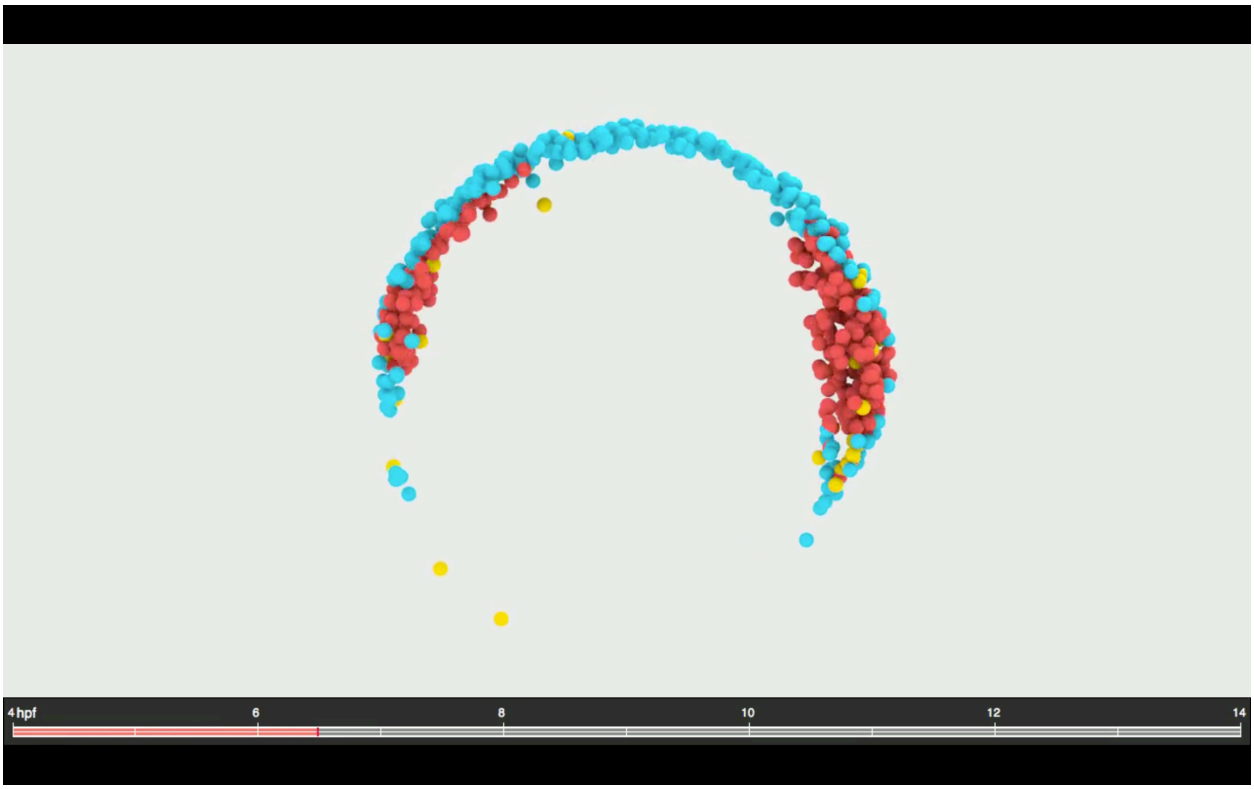

Movie S3: Radial and latitudinal cell organization at body axis.

View of the zebrafish body-axis showing radial and latitudinal organization of germlayers. Cell centroids rendered as solid spheres, with cells belonging to p. ectoderm (blue), mesendoderm (red) and endoderm (yellow).

(Submitted videos have been compressed to stay within the file size limits. Higher quality movies are available at https://cloud.mpi-cbg.de/index.php/s/YuKBKB6WPwXRCmA)

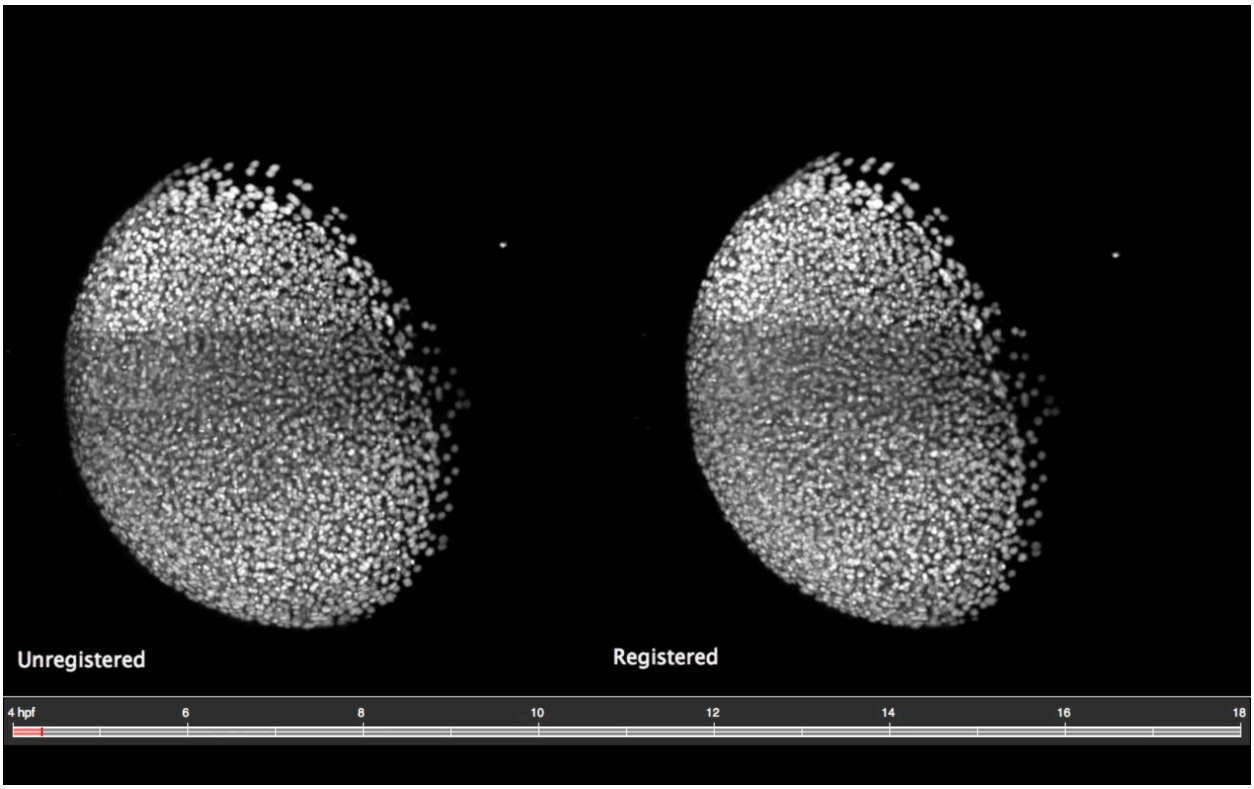

Movie S4: Registration of embryo to eliminate global movement

Images at two consecutive time-points of the movie are aligned with each other to eliminate any global movement of the embryo itself and to preserve local cell movements. This movie compares the unregistered (left) and registered (right) data.

(Submitted videos have been compressed to stay within the file size limits. Higher quality movies are available at https://cloud.mpi-cbg.de/index.php/s/YuKBKB6WPwXRCmA)

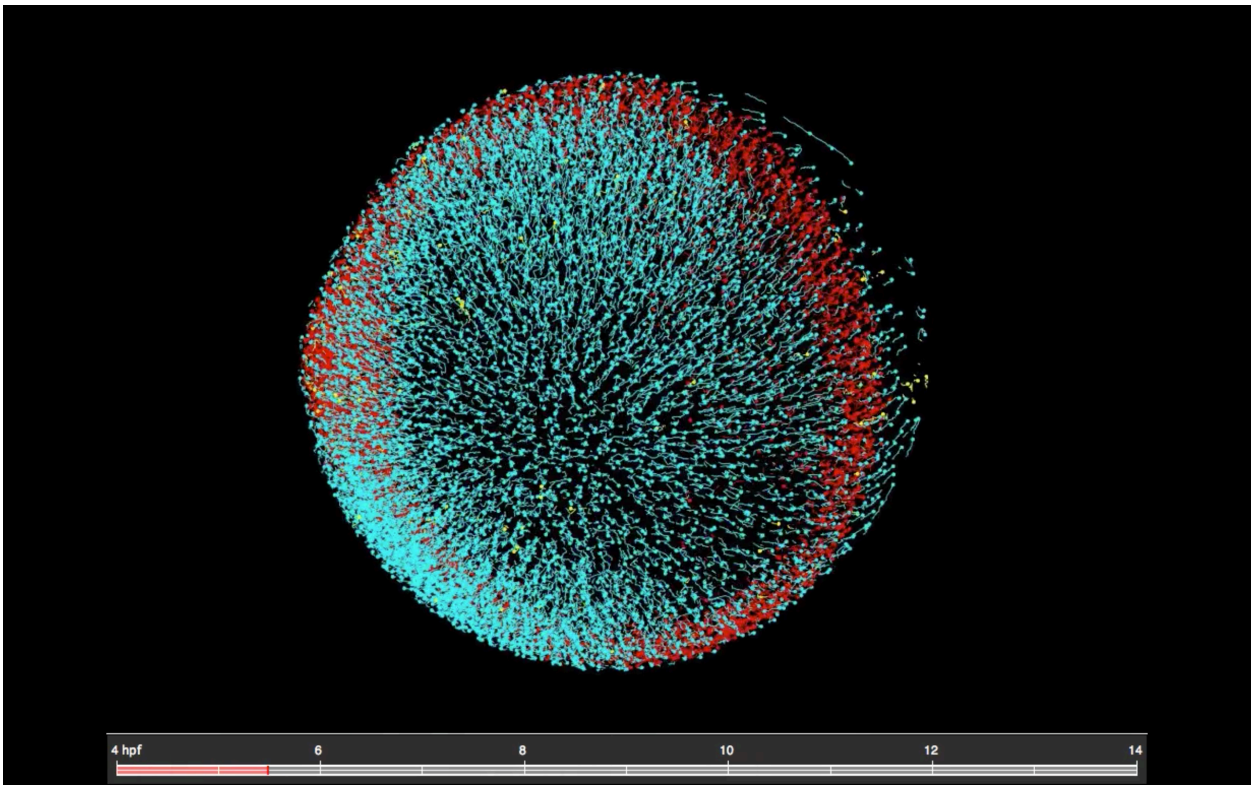

Movie S5: Cell tracking of all germlayers merged

Extracted cell trajectories between 4 hpf and 14 hpf. Tracks of p. ectoderm (blue), mesendoderm (red) and endoderm (yellow). The current cell position is shown as a filled circle and the positions over the past 10 time points (corresponding to 20 mins) as the trail of each track.

(Submitted videos have been compressed to stay within the file size limits. Higher quality movies are available at https://cloud.mpi-cbg.de/index.php/s/YuKBKB6WPwXRCmA)

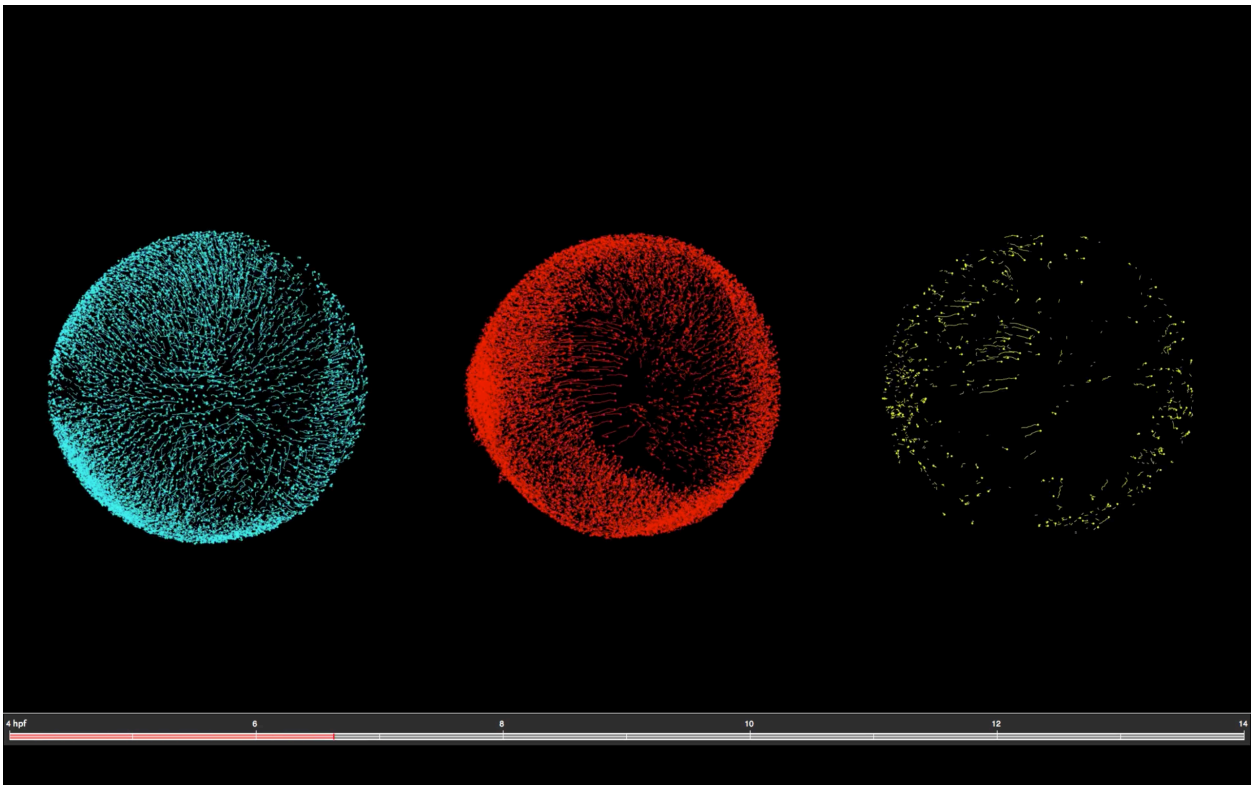

Movie S6: Cell tracking of all layers separated

Extracted cell trajectories between 4 hpf and 14 hpf. Tracks of p. ectoderm (blue - left), mesendoderm (red - middle) and endoderm (yellow - right) are shown in separate views. Current cell position is shown as a filled circle and the positions over the past 10 time points (corresponding to 20 mins) as the trail of each track.

(Submitted videos have been compressed to stay within the file size limits. Higher quality movies are available at https://cloud.mpi-cbg.de/index.php/s/YuKBKB6WPwXRCmA)